Cerebral blood flow predicts differential neurotransmitter activity

Juergen Dukart[1], Štefan Holiga[1], Christopher Chatham[1], Peter Hawkins[2], Anna Forsyth[3], Rebecca McMillan[3], Jim Myers[8], Anne R Lingford-Hughes[8], David J Nutt[9], Emilio Merlo-Pich[1], Celine Risterucci[1], Lauren Boak[1], Daniel Umbricht[1], Scott Schobel[1], Thomas Liu[4], Mitul A Mehta[2], Fernando O Zelaya[2], Steve C Williams[2], Gregory Brown[5], Martin Paulus[5], Garry D Honey[1], Suresh Muthukumaraswamy[3], Joerg Hipp[1], Alessandro Bertolino[1,6], Fabio Sambataro[1,7]

[1] *F. Hoffmann-La Roche, pharma Research Early Development, Roche Innovation Centre Basel, Basel, Switzerland.*

[2] *Department of Neuroimaging, Institute of Psychiatry, Psychology & Neuroscience, King's College London, London, United Kingdom*

[3] *School of Pharmacy, Faculty of Medical and Health Sciences, The University of Auckland, Auckland, New Zealand*

[4] *Center for Functional MRI, University of California San Diego, 9500 Gilman Drive MC 0677, La Jolla, CA 92093, United States; Departments of Radiology, Psychiatry and Bioengineering, University of California San Diego, 9500 Gilman Drive, La Jolla, CA 92093, United States. Department of Psychiatry*

[5] *University of California, San Diego, La Jolla, USA Veterans Affairs San Diego Healthcare System, San Diego, USA*

[6] *Institute Of Psychiatry, Department of Basic Medical Science, Neuroscience and Sense Organs, University of Bari 'Aldo Moro'*

[7] *Department of Experimental and Clinical Medical Sciences (DISM), University of Udine, Udine, Italy*

[8] *Centre for Neuropsychopharmacology, Imperial College London, London, United Kingdom*

[9] *Department of Medicine, Centre for Neuroscience, Imperial College London, London, UK*

Short title: CBF predicts differential neurotransmitter activity

Word count abstract/introduction/discussion/article: 148/603/1313/4358 (w/o references & tables)

Corresponding author:

Juergen Dukart, PhD

Biomarkers & Clinical Imaging, Translational Medicine Neuroscience

F. Hoffmann-La Roche

Grenzacherstrasse 170

4070 Basel

Switzerland

Email: juergen.dukart@gmail.com

Phone: +41 (0)61 68 77091

Fax: +41 61 68 79848

Abstract

Application of metabolic magnetic resonance imaging measures such as cerebral blood flow in translational medicine is limited by the unknown link of observed alterations to specific neurophysiological processes. Here we address this question by probing cerebral blood flow in healthy volunteers using seven established drugs with known dopaminergic, serotonergic, glutamatergic and GABAergic mechanisms of action in a novel framework aimed at disentangling the observed effects to underlying neurotransmitter systems. We find for all evaluated compounds a reliable spatial link of respective cerebral blood flow changes with underlying activity and/or neurotransmitter receptor densities corresponding to their primary mechanisms of action. The strength of these associations with receptor density is mediated by respective drug affinities. These findings validate cerebral blood flow as a sensitive brain-wide in-vivo assay of metabolic demands across a variety of neurotransmitter systems in humans, with widespread implications for translational medicine and drug discovery alike.

Significance statement

Whilst magnetic resonance imaging of cerebral blood flow is commonly applied for studying human brain disease and therapeutic interventions it remains obscure if and how such measures reflect specific underlying neurophysiological activity or disease pathology in specific neurotransmitter systems. Here we examine the effects of seven drugs with differential dopaminergic, serotonergic, glutamatergic and GABAergic mechanisms of action on cerebral blood flow. We demonstrate that cerebral blood flow closely reflects specific activity changes from various underlying neurotransmitter systems. These findings and the proposed framework have widespread implications for deploying metabolic magnetic resonance imaging measures for a more informative evaluation of disease pathology and different therapeutic interventions.

Introduction

Metabolic task-based and resting state magnetic resonance imaging (MRI) of blood oxygen level dependence and cerebral blood flow (CBF) are now commonly applied for studying human brain function, disease pathology and for evaluation of pharmacodynamic (PD) effects associated with pharmacological interventions (Borsook et al., 2006; Matthews et al., 2006; Greicius et al., 2007; Logothetis, 2008; Petcharunpaisan et al., 2010; Wise and Preston, 2010; Calhoun et al., 2011; Wang et al., 2011; Detre et al., 2012). In particular, state of the art arterial spin labeling (ASL) sequences now allow for quantitative CBF evaluation (Alsop et al., 2015). Despite their wide-spread applications in healthy and diseased populations there is limited understanding of whether and how metabolic effects measured through these techniques reflect underlying activity in specific neurotransmitter systems (Matthews et al., 2006; Logothetis, 2008; Petcharunpaisan et al., 2010; Wise and Preston, 2010; Roffman et al., 2016). A better understanding could unveil potential mechanisms of disease and crucial components of complex drug action that underpin functional modulation (Logothetis, 2008; Singh, 2012). Major limitations discussed in that context are potential contributions of confounding physiological, e.g. cardiovascular effects, unclear association with specific neurotransmitter systems and agonist and antagonist effects and a narrow cross-species translational value restricting comparisons to a descriptive anatomical level (Agelink et al., 2001; Volkow et al., 2003; Choi et al., 2006; Shmueli et al., 2007; Wu et al., 2009; Thase et al., 2013; Seah et al., 2014; Bruns et al., 2015; Francois et al., 2016). Addressing those limitations is therefore key to wide-spread application of metabolic MRI in translational medicine.

Receptor theory provides a possible way of addressing these limitations (Danhof et al., 2008; Logothetis, 2008). This theory posits that relationships between drug kinetics and observed PD effects depend on both the drug (i.e. receptor affinity and mechanism of action) and the biological system (i.e. receptor density and activity). Based on this concept drugs affecting specific receptor systems should lead to higher metabolic changes in regions with higher respective receptor densities. The strength of this relationship should be further dependent on the affinity of the compounds to the respective receptor systems. However, this assumption only partially holds for drugs with an indirect mechanism of action (i.e. allosteric modulators and reuptake inhibitors). As such drugs do not directly induce activation but rather facilitate its effects one would expect their effects to co-localize with underlying activity. In contrast, direct a(nta)gonists should additionally also activate yet inactive regions with high respective receptor densities.

Using this concept, we assess if ASL derived CBF changes (ΔCBF) induced by seven established compounds with known direct or indirect dopaminergic, serotoninergic, glutamatergic and/or GABAergic mechanisms of action (escitalopram, methylphenidate, haloperidol, olanzapine, low and high dose of risperidone, ketamine and midazolam, Table 1) are associated with respective receptor densities, underlying activity and affinities to the respective receptor types (Figure 1). Based on the above considerations, we hypothesize stronger ΔCBF in regions with higher respective receptor densities in particular for drugs with a direct mechanism of action and to a weaker extent for allosteric modulators and reuptake inhibitors. Furthermore, we expect stronger ΔCBF in regions with higher underlying activity for both compounds with direct (direct agonists and antagonists) and indirect mechanisms of action (allosteric modulators and reuptake inhibitors). Lastly, we hypothesize the association strength between ΔCBF and receptor densities to be dependent on the respective drug affinities. We test those hypotheses by first evaluating the link between drug-induced ΔCBF with ex vivo and in vivo estimates of different receptor densities and expected underlying activity. In a second step we then test if the association strength of these relationships is dependent on the respective drug affinities.

Materials and Methods

[Table 1]

[Figure 1]

Subject and study details

Data from 5 studies, all in young healthy volunteers, were included. An overview of all studies including medication and dosing details is provided in Table 1. All studies were part of a coordinated effort by F.Hoffmann-La Roche to collect CBF data from drugs with different mechanisms of action following similar fully counter-balanced, placebo controlled, cross-over designs. Adaptations of study designs were performed for each study to account for different administration modes, wash-out times and pharmacokinetic/pharmacodynamic profiles of the evaluated compounds. All studies were approved by local ethics committees. Study 1 and 2 were conducted using a double-blind, randomized, three-period (each one week apart) cross-over design. Study 1 included three imaging sessions following single dose administration of either low or high dose of risperidone or placebo. Similarly, study 2 included three imaging sessions following single dose administration of olanzapine, haloperidol or placebo. Study 3 was

executed in a double-blind, single dose, randomized, four period (each two weeks apart) cross-over design. Evaluated drugs were methylphenidate, escitalopram, a Roche investigational compound (a glutamatergic subtype modulator whose development was terminated, data not reported here) and placebo. Study 4 was a single-blind, randomized, three period cross-over study with imaging performed following intravenous administration of ketamine, midazolam or placebo. Study 5 was a non-treatment test-retest study comprising three MRI visits each including ASL. This study was used as a negative control dataset and to derive activity estimates for the drug studies. Dose selection for all drugs was performed based on the expected receptor occupancy, expected behavioral effects and safety and tolerability considerations. A detailed description of the mechanisms of action for all compounds is provided in Table 1 and Supplement 1.

ASL data

Image acquisition onset for each study was based on the expected PK maximum for the corresponding compounds (2 hours post dose for Study 1, 5 hours post dose for Study 2, 4 hours post dose for Study 3). ASL data with varying sequences) were acquired for all studies and all visits among other study specific imaging modalities. For Study 1 and 2 two runs of ASL were acquired at each session. For these studies, run 2 data of each session were used for primary analyses to reduce potential arousal effects at the beginning of the acquisition. Details on ASL acquisition and preprocessing of resulting cerebral blood flow data are provided in Supplement 1 (Supplementary methods and Supplementary Table 1). Due to lack of identical ASL sequences for different manufacturers and scanner types, the best available scanner-specific ASL protocol at the time of study conduct was used for each study.

Receptor density maps

Receptor density maps for 41 regions (Brodmann areas and subcortical nuclei) were extracted for the following 13 receptor types from the publication by Palomero-Gallagher et al. (Palomero-Gallagher et al., 2015) using a coarse scale provided by the authors: for glutamate (AMPA, NMDA and Kainate), for GABA (GABAa), for acetylcholine and muscarine (M1 and M2), for nicotine (nicotinic α4/β2), for catecholamines (α1 and α2), for serotonin (5-HT 1A and 5-HT 2), for dopamine (D1 and D2) (Supplementary Table 2). Brodmann regions have been shown to provide distinct functional information as measured through resting state MRI if at all rather under-parcellating such data (Gordon et al., 2014). A detailed description of receptor density map extraction is provided in Supplement 1.

As these coarse receptor density maps were obtained from a review publication of ex vivo studies, we aimed to additionally evaluate if more fine grained in vivo density estimates provided by molecular receptor imaging further improve the observed associations. For this we extracted dopamine transporter (DAT) and GABAa density estimates as measured through DAT-SPECT and flumazenil PET for the 41 regions reported above. DAT-SPECT data were obtained from a publicly available control cohort of healthy volunteers (Parkinson's Progression Marker Initiative) (Figure 3B). GABAa density estimates were obtained using flumazenil PET data of 6 healthy volunteers acquired at the Imperial College London. Details on these cohorts, pre-processing and DAT and GABAa density estimation are provided in Supplement 1.

Pharmacodynamic CBF profiles

A Brodmann area map as included in the MRIcron tool (Rorden and Brett, 2000) was normalized into the Montreal Neurological Institute space using the Statistical Parametric Mapping (SPM12) normalize function (Friston et al., 1994). For putamen, caudate and fusiform gyrus regions the corresponding automated anatomical labeling atlas regions were used. Mean CBF values were extracted for drug and placebo images from the 41 regions corresponding to Brodmann and subcortical areas covered by the receptor density maps described above. A ΔCBF profile for each drug was calculated as an effect size per region for the whole group by computing the average regional drug-induced change across all subjects divided by the standard deviation of the change in the respective region (Figure 2B and Supplementary Figure 4). Effect size was chosen to minimize the potential impact of between region differences in signal to noise but also due to site, scanner and sequence differences across different studies. For Study 5, test retest data of each subject for visit 1 and 2 were randomly assigned to either drug or placebo condition.

CBF activity maps

To evaluate if drug-induced ΔCBF is also linked to underlying activity we used the non-drug study 5 data from all visits to compute a quantitative average CBF map (Figure 1). Mean CBF values extracted from this map for the 41 regions introduced above were used as independent expected activity estimates for the respective regions for all drug data.

Mapping ΔCBF ***to receptor densities***

For interpretation of subsequent correlations between receptor density and ΔCBF maps we first aimed to understand if and how the obtained receptor maps provide similar or differential information regarding spatial receptor density distribution. Pearson correlations and coefficients of determination were computed between each pair of receptor density maps to estimate their association strength. Validity of the parametric statistics described below (parametric and normality assumptions for Pearson correlations and multiple linear regression models) was established using permutation statistics and Shapiro-Wilk tests for normality (s. Supplementary methods and results for description and outcomes of those analyses). Additionally, to further ensure that the choice of parametric tests did not bias the results we repeated all analyses using Spearman correlation coefficients (Figure S5).

We next aimed to understand if and how receptor density maps are linked to observed drug-induced ΔCBF profiles (1) separately for each receptor type and (2) whilst controlling for the variance explained by other receptor density maps. For these we performed two types of analyses: (1) simple Pearson correlations between each receptor density map and each ΔCBF map and (2) multiple linear regression models using each ΔCBF map as a dependent variable and including all receptor maps as covariates. For analysis (1) we report if correlations survive strict Bonferroni correction (accounting for the number of tests performed per compound) and additionally as exploratory findings all correlations surviving an uncorrected $p<.05$. For analysis (2) to reduce data loss due to missing values the interpolated receptor density maps described in Supplement 1 were used. To ensure that the interpolation did not bias the results, this analysis was repeated using the initial receptor density maps excluding regions with missing values (s. Supplementary results). In analysis (2) we test for significance of each overall model and the single regressors to predict ΔCBF profiles ($p<.05$).

We then tested if continuous in vivo receptor density estimates further improve the associations between receptor densities and ΔCBF. For this we computed for all compounds with known dopaminergic mechanism correlation coefficients with DAT density estimates obtained through DAT-SPECT. Similarly, we computed for midazolam being the only GABAergic compound its correlation with flumazenil-based GABAa receptor density estimates. To ensure that the putative outlier region showing a very low GABAa expression (Figure 3c) did not bias the results we further repeated the correlation analysis with GABAa using non-parametric Spearman correlation coefficient with all data and after the removing the outlier.

Lastly, as several ASL acquisitions were available for some of the compounds, we used those data to evaluate the test-retest reliability of the above relationships between ΔCBF and receptor densities (s. Supplement 1 for description and detailed outcomes of those analyses).

Testing for associations with underlying activity

Similarly to the above associations with receptor density we followed a two-step procedure to test if drug-induced ΔCBF is associated with expected activity profile. In a first analysis, we tested for associations between activity profile and ΔCBF using Pearson correlations. We then tested using multiple linear regressions if these relationships still hold when controlling for the contributions of significant receptor density regressors identified above.

Testing for associations with receptor affinity

To further understand if the observed relationships between receptor densities and ΔCBF are also associated with the respective receptor affinities (Ki) we first extracted the affinities for compounds with direct receptor binding mechanism of action established using the same methodology (risperidone, olanzapine and haloperidol) from Bymaster et al. (Supplementary Table 3) (Bymaster et al., 1996). We then correlated these log transformed affinities with the observed ΔCBF to receptor density correlational profiles for each drug (pooled and separately for each compound). A more detailed description of this analysis is provided in Figure 1 and Supplement 1.s

Results

Cerebral blood flow changes correlate with receptor densities

Receptor density maps extracted from a review publication by Palomero-Galagher et al. (Palomero-Gallagher et al., 2015) showed a low average co-localization; in addition, compounds with different mechanisms of action also showed low similarity of drug-induced CBF patterns (Figure 2B, Supplementary results, Figure S2 and S3).

[Figure 2]

We then tested for direct relationships between drug-induced ΔCBF and underlying receptor density maps using correlational analysis. For all compounds beside the GABAergic positive allosteric modulator midazolam we find drug-induced ΔCBF to be consistently correlated with receptor densities corresponding to the known mechanisms of action of the respective drugs (Figure 2A, Table 1). For

example, the serotonin agonist escitalopram showed the strongest correlation with serotonergic 5-HT 2 receptor. Consistently, dopamine antagonists risperidone and haloperidol showed significant correlations with D1 and/or D2 receptor densities. Similarly, also olanzapine, methylphenidate and ketamine showed significant correlations (though not all survived Bonferroni correction) with receptor densities corresponding to their known dopaminergic, serotonergic and glutamatergic mechanisms of action. The results of non-parametric analyses using Spearman correlation coefficients were largely similar to the parametric analysis outcomes (Figure S5).

[Figure 3]

As the above correlational analyses are based on coarse ex vivo receptor density estimates (Palomero-Gallagher et al., 2015), we aimed to evaluate if more fine-grained in vivo density estimates as obtained using molecular receptor imaging of DAT and GABAa are more sensitive for identifying such associations. These correlational analyses revealed very strong and highly significant positive correlations with DAT for the dopamine antagonists haloperidol, olanzapine, and both low and high dose of risperidone but not for the reuptake inhibitor methylphenidate (Figure 3a). Correlation of ΔCBF obtained for the positive allosteric modulator midazolam with flumazenil-based GABAa receptor density estimates revealed a weak but significant association between both (Figure 3c). This correlation remained significant using Spearman correlation coefficient on all data (rho=-.43;p=.005) and after removing the outlier (rho=-.39;p=.013).

Distinct contribution of different receptor systems to cerebral blood flow changes

Whilst the above correlational analyses provide an estimate of the direct association strength between two measures they do not account for correlations between receptor densities and/or may miss potential weaker associations in presence of a strong effect. Multiple linear regression analyses address these limitations although this is at the cost of a potentially lower sensitivity when regressors are strongly correlated and/or explain similar variance in the dependent variable. To evaluate the distinct contributions of each receptor map to the drug induced ΔCBF and to test for additional associations not discovered through correlational analyses, we therefore computed multiple linear regressions including all receptor densities as regressors in the same model. Significant model fits were observed for all evaluated drugs beside midazolam and the negative control dataset (escitalopram: F(13,27)=2.7;p=.015, haloperidol: F(13,27)=3.2;p=.005, risperidone (low dose): F(13,27)=3.6;p=.002, risperidone (high dose):

F(13,27)=5.0;p<.001, olanzapine: F(13,27)=2.8;p=.011, methylphenidate: F(13,27)=3.7;p=.002, ketamine: F(13,27)=2.4;p=.027, midazolam: F(13,27)=1.4;p=.219, negative control: F(13,27)=1.5;p=.175).

To identify which neurotransmitter maps contributed most to these model fits, we then evaluated the significance of each receptor density regressor (Figure 2). These analyses largely replicate the correlational findings and provide evidence of a distinct contribution of the different receptor density maps to the drug-induced ΔCBF. Additionally, they reveal further significant noradrenergic and/or serotonergic contributions for methylphenidate and olanzapine, consistent with their known mechanisms of action. Despite the non-significant overall model fit for midazolam, GABAa was the only significant single receptor density regressor for this compound, in line with midazolam's mechanism of action.

To assess the robustness of the obtained correlational and multiple regression profiles linking ΔCBF to receptor densities, we evaluated the test-retest reliabilities for compounds where more than one CBF acquisition was available for each subject (risperidone, olanzapine and haloperidol). The association strengths of ΔCBF to receptor density showed excellent test-retest reliability both within and between sessions (intra class correlation coefficients between 0.83 and 0.99; Supplementary results).

Cerebral blood flow changes correlate with underlying activity

Having established the link between ΔCBF and receptor densities for the respective compounds we then aimed to understand if underlying activity is also a predictor of PD effects on CBF. For this we computed correlation coefficient between expected underlying activity and observed ΔCBF for each compound. We observed significant associations between both for midazolam (r=-.48;p=002), methylphenidate (r=-.56;p<.001), haloperidol (r=-.52;p<.001), olanzapine (r=-.62;p<.001), low (r=-.34;p=.028) and high (r=-.57;p<.001) dose of risperidone, a marginally significant effect for escitalopram (r=-.30;p=.055) and no significant effect for ketamine (r=.02;p=.913). When adjusting for the variance explained by receptor densities showing a significant association with respective compounds the effect of underlying activity remained significant for all compounds except escitalopram and ketamine (midazolam: p=.003; methylphenidate: p=.033; haloperidol: p<.001; olanzapine: p<.001; risperidone low dose: p=.050; risperidone high dose: p<.001; escitalopram: p=.471; ketamine: p=.585).

Strength of CBF to receptor density associations is linked to respective receptor affinities

Whereas the above correlational and multiple linear regression analyses provide evidence of distinct and reliable associations between drug-induced ΔCBF and underlying receptor densities, they remain descriptive with respect to consistency of the observed associations with the respective mechanisms of action of the evaluated compounds. We formally tested this hypothesis by evaluating if the observed association strength profiles between ΔCBF and receptor densities can be explained by drug affinities to the corresponding receptor systems. In a pooled analysis across the three drugs for which the affinity was established using the same methodology we find a highly significant correlation ($p<.001$) between the obtained profiles and the respective receptor affinities (Figure 3d). Separate tests for each compound confirmed these significant associations for haloperidol and risperidone.

Discussion

Here we evaluated for seven established compounds acting on dopamine, serotonin, catecholamine, glutamate and GABA the relationship between respective ΔCBF and receptor densities of the underlying neurotransmitter systems. For all compounds, with six out of seven being significant, we find direct and distinct spatial relationships between drug-induced ΔCBF and underlying receptor densities and activity. Moreover, in line with assumptions derived from receptor theory we show that the association strength of these relationships is dependent on the affinity of the drugs to the underlying receptor systems (Danhof et al., 2008).

More specifically, for all evaluated serotonin antagonists we find positive associations between serotonergic system as represented by 5-HT 1a and 2 receptors and drug-induced ΔCBF. These findings suggest that inhibition of this system may be associated with a net increased metabolic demand in the corresponding regions. A more complex picture was observed for serotonin agonists. Whilst ΔCBF induced by both reuptake inhibitors showed a significant negative association with 5-HT 2 receptor density, ketamine showed a significant positive association with this receptor in line with its direct agonist effect on serotonin (Kapur and Seeman, 2002; Carhart-Harris et al., 2012). This finding suggests interactions between observed ΔCBF and underlying receptor systems, e.g. due to differential effects of orthosteric and allosteric agonists or due to the commonly reported interdependence of dopaminergic, serotonergic and glutamatergic systems (Green and Grahame-Smith, 1974; Kuczenski and Segal, 1989; Moghaddam et al., 1997; Mendlin et al., 1999).

In contrast, all dopamine agonists as well as antagonists evaluated here showed a significant positive association with the underlying D1 and/or D2 receptor densities suggesting a U-shaped association of

dopamine levels and metabolic demand. These findings are consistent with previous research reporting increased striatal CBF after administration of both dopamine agonists and antagonists (Mu et al., 2007; Fernández-Seara et al., 2011; Handley et al., 2013; Schouw et al., 2013). These findings imply that the hypothesized U-shaped curve relating dopamine to cognitive performance may be paralleled by a U-shaped curve relating dopamine to metabolic demand; for example, cognitive function might improve if dopamine levels are titrated to minimize resting metabolic demands in substrates most strongly associated with those functions(Arnsten, 2011; Cools and D'Esposito, 2011). Supportive for these findings with respect to dopamine are also the strikingly strong correlations observed for all three direct dopamine antagonists with in vivo DAT receptor density estimates being a close surrogate of ex vivo counts of dopaminergic neurons (Kraemmer et al., 2014). The strength of these associations with DAT estimates was substantially increased for the high as compared to low dose of risperidone suggesting dose dependency of the observed associations.

Similarly, the ketamine induced ΔCBF profile was significantly correlated with NMDA (though not surviving Bonferroni correction in the parametric analysis), 5-HT and several other receptor systems including AMPA, for which a ketamine related mechanism of action has only recently been discovered (Kapur and Seeman, 2002; Zanos et al., 2016). Though for the GABAergic positive allosteric modulator midazolam the overall model was not significant the finding of GABAa receptor density being the only significant regressor in the multiple linear regression analysis is in line with its expected mechanism of action. In line with this, *in vivo* estimates of GABAa obtained through flumazenil PET also showed a significant association. Nevertheless, despite reaching significance the association strength with GABAa for midazolam remains weak. This observation is in line with its positive allosteric mechanism of action that would predict its effects to be primarily co-localized with the underlying activity of the system (Changeux, 2013). Indeed, we find for midazolam and all other compounds with an indirect mechanism of action significant associations between ΔCBF and underlying activity estimates. The strong correlation observed for methylphenidate in that context also explains its weak correlation with DAT to which it directly binds. With a similar argumentation as for midazolam methylphenidate requires activity to take place to exhibit its pharmacological effect. Moreover, in line with our hypothesis we find underlying activity to be also a significant contributor to PD profiles for all compounds with a direct mechanism of action except ketamine. Potential reasons for the lack of such an association for ketamine might be in its wide-spread anesthetic effects that could interfere or alter underlying resting state activity patterns making the applied activity estimates imprecise (Anon, n.d.).

Supportive for the idea that the established associations between receptor densities and ΔCBF indeed reflect the primary mechanisms of action of the respective compounds are the observed significant correlations of these profiles with respective receptor affinities in the pooled analysis, and also separately for haloperidol and risperidone.

That said, several unexpected findings emerged from our analyses that may relate to limitations of the proposed approach. For example, we do not observe significant associations of escitalopram induced ΔCBF with 5-HT 1a receptor density or between methylphenidate ΔCBF and D1 or DAT receptor density. These negative findings may be false negatives, but may alternatively relate to an important commonality between these compounds: their indirect mechanism of action. Both drugs act as reuptake inhibitors. They therefore require some underlying activity to facilitate its effects. These negative findings may therefore also indicate a relatively low activity of the associated receptor systems at rest. In line with this potential explanation are also the observed significant associations observed for both compounds with the underlying activity estimates. Similarly, despite a high affinity of olanzapine to the M1 receptor we do not observe a significant association between both. This negative finding could suggest a reduced sensitivity of ΔCBF to activity changes related to muscarinic system. However, contrary to this assumption we observe a significant association between M1 and ketamine induced ΔCBF that is also known to have a high affinity to the respective receptor. Among other such discrepant findings may also arise from different scanner types and ASL sequences used for evaluation of different compounds leading to differential sensitivity to detect respective associations.

Differences in observed associations may also arise from the applied drug dosing and frequency. For example, higher dosing may be expected to result in a higher proportion of secondary targets occupied by the drug. Similarly, some PD effects may evolve on a slower temporal scale. Lastly, we also observe some significant associations between drug-induced ΔCBF and receptor systems with known low affinity of the respective compounds. In example, a significant association is observed between methylphenidate induced ΔCBF and serotonergic system despite its low affinity to serotonergic receptors (Markowitz et al., 2009). As the applied correlational approach does not differentiate between direct and indirect effects the observed associations may well reflect some previously reported indirect effects of dopaminergic stimulation on the serotonin system (Gainetdinov et al., 1999; Daw et al., 2002).

In summary, our results provide strong evidence that CBF reflects specific metabolic demands from diverse underlying neurotransmitter systems. We further demonstrate that the proposed approach allows for disentangling of PD effects on CBF to underlying receptor densities and activity, in most cases

closely reflecting the mechanisms of action of the respective compounds. With the additionally demonstrated excellent reliability of obtained CBF to receptor density profiles, these findings further strengthen the value of CBF as a sensitive brain-wide in-vivo assay of metabolic demands across a variety of neurotransmitter systems in humans and promising tool for drug development and disease evaluation (Borsook et al., 2006; Petcharunpaisan et al., 2010; Wise and Preston, 2010; Wang et al., 2011; Bruns et al., 2015). In particular in drug development, the proposed approach may be used to generate data-driven hypothesis about the pharmacodynamic mechanisms of action of novel but also established compounds. Though subject to evaluation the proposed receptor density mapping approach may provide an easy implementable framework for application to other functional neuroimaging measures (Krystal and Weiner, 1999; Logothetis, 2008; Singh, 2012; Roffman et al., 2016) and allows a direct integration of in vivo receptor density estimates as provided by molecular imaging (Paterson et al., 2013; Kaufman et al., 2015; Beliveau et al., 2016).

Acknowledgments

DAT-SPECT data used in the preparation of this article were obtained from the Parkinson's Progression Markers Initiative (PPMI) database (www.ppmi-info.org/data). For up-to-date information on the study, visit www.ppmi-info.org. PPMI – a public-private partnership – is funded by the Michael J. Fox Foundation for Parkinson's Research and funding partners, including Abbvie, Avid Radiopharmaceuticals, Biogen Idec, Briston-Myers Squibb, Covance, GE Healthcare, Genentech, GlaxoSmithKline, Lilly, Lundbeck, Merck, Meso Scale Discovery, Pfizer, Piramal, Roche and UCB.

Funding and Disclosure

JD, SH, CH, CR, DU, LB, GH, JH, AB and FS are current or former full-time employees of F.Hoffmann-La Roche, Basel Switzerland. The authors received no specific funding for this work. F.Hoffmann-La Roche provided financial contribution in the form of salary for all authors listed above but did not have any additional role in the study design, data collection and analysis, decision to publish, or preparation of the manuscript.

PH, AF, RM, JM, ARL, DJN, TL, MAM, FOZ, SCW, GB, MP and SM report no conflicts of interest.

References

Agelink MW, Majewski T, Wurthmann C, Lukas K, Ullrich H, Linka T, Klieser E (2001) Effects of newer atypical antipsychotics on autonomic neurocardiac function: a comparison between amisulpride, olanzapine, sertindole, and clozapine. J Clin Psychopharmacol 21:8–13.

Alsop DC, Detre JA, Golay X, Günther M, Hendrikse J, Hernandez-Garcia L, Lu H, MacIntosh BJ, Parkes LM, Smits M (2015) Recommended implementation of arterial spin-labeled perfusion MRI for clinical applications: A consensus of the ISMRM perfusion study group and the European consortium for ASL in dementia. Magn Reson Med 73:102–116.

Anon (n.d.) Ketamine: Teaching an Old Drug New Tricks : Anesthesia & Analgesia. LWW Available at: http://journals.lww.com/anesthesia-analgesia/Fulltext/1998/11000/Ketamine__Teaching_an_Old_Drug_New_Tricks.39.aspx [Accessed November 22, 2016].

Arnsten AF (2011) Catecholamine influences on dorsolateral prefrontal cortical networks. Biol Psychiatry 69:e89–e99.

Beliveau V, Ganz M, Feng L, Ozenne B, Højgaard L, Fisher PM, Svarer C, Greve DN, Knudsen GM (2016) A high-resolution in vivo atlas of the human brain's serotonin system. J Neurosci:2830–16.

Borsook D, Becerra L, Hargreaves R (2006) A role for fMRI in optimizing CNS drug development. Nat Rev Drug Discov 5:411–425.

Bruns A, Mueggler T, Künnecke B, Risterucci C, Prinssen EP, Wettstein JG, von Kienlin M (2015) "Domain gauges": A reference system for multivariate profiling of brain fMRI activation patterns induced by psychoactive drugs in rats. NeuroImage 112:70–85.

Bymaster FP, Calligaro DO, Falcone JF, Marsh RD, Moore NA, Tye NC, Seeman P, Wong DT (1996) Radioreceptor binding profile of the atypical antipsychotic olanzapine. Neuropsychopharmacology 14:87–96.

Calhoun VD, Sui J, Kiehl K, Turner J, Allen E, Pearlson G (2011) Exploring the psychosis functional connectome: aberrant intrinsic networks in schizophrenia and bipolar disorder. Front Psychiatry 2.

Carhart-Harris RL, Erritzoe D, Williams T, Stone JM, Reed LJ, Colasanti A, Tyacke RJ, Leech R, Malizia AL, Murphy K, Hobden P, Evans J, Feilding A, Wise RG, Nutt DJ (2012) Neural correlates of the psychedelic state as determined by fMRI studies with psilocybin. Proc Natl Acad Sci 109:2138–2143.

Changeux J-P (2013) The concept of allosteric modulation: an overview. Drug Discov Today Technol 10:e223–e228.

Choi J-K, Chen YI, Hamel E, Jenkins BG (2006) Brain hemodynamic changes mediated by dopamine receptors: Role of the cerebral microvasculature in dopamine-mediated neurovascular coupling. NeuroImage 30:700–712.

Cools R, D'Esposito M (2011) Inverted-U–shaped dopamine actions on human working memory and cognitive control. Biol Psychiatry 69:e113–e125.

Danhof M, de Lange ECM, Della Pasqua OE, Ploeger BA, Voskuyl RA (2008) Mechanism-based pharmacokinetic-pharmacodynamic (PK-PD) modeling in translational drug research. Trends Pharmacol Sci 29:186–191.

Daw ND, Kakade S, Dayan P (2002) Opponent interactions between serotonin and dopamine. Neural Netw 15:603–616.

Detre JA, Rao H, Wang DJJ, Chen YF, Wang Z (2012) Applications of arterial spin labeled MRI in the brain. J Magn Reson Imaging 35:1026–1037.

Fernández-Seara MA, Aznárez-Sanado M, Mengual E, Irigoyen J, Heukamp F, Pastor MA (2011) Effects on resting cerebral blood flow and functional connectivity induced by metoclopramide: a perfusion MRI study in healthy volunteers. Br J Pharmacol 163:1639–1652.

Francois J, Grimm O, Schwarz AJ, Schweiger J, Haller L, Risterucci C, Böhringer A, Zang Z, Tost H, Gilmour G, Meyer-Lindenberg A (2016) Ketamine Suppresses the Ventral Striatal Response to Reward Anticipation: A Cross-Species Translational Neuroimaging Study. Neuropsychopharmacology 41:1386–1394.

Friston KJ, Holmes AP, Worsley KJ, Poline J-P, Frith CD, Frackowiak RS (1994) Statistical parametric maps in functional imaging: a general linear approach. Hum Brain Mapp 2:189–210.

Gainetdinov RR, Wetsel WC, Jones SR, Levin ED, Jaber M, Caron MG (1999) Role of Serotonin in the Paradoxical Calming Effect of Psychostimulants on Hyperactivity. Science 283:397–401.

Gordon EM, Laumann TO, Adeyemo B, Huckins JF, Kelley WM, Petersen SE (2014) Generation and evaluation of a cortical area parcellation from resting-state correlations. Cereb Cortex:bhu239.

Green AR, Grahame-Smith DG (1974) The role of brain dopamine in the hyperactivity syndrome produced by increased 5-hydroxytryptamine synthesis in rats. Neuropharmacology 13:949–959.

Greicius MD, Flores BH, Menon V, Glover GH, Solvason HB, Kenna H, Reiss AL, Schatzberg AF (2007) Resting-state functional connectivity in major depression: abnormally increased contributions from subgenual cingulate cortex and thalamus. Biol Psychiatry 62:429–437.

Handley R, Zelaya FO, Reinders AATS, Marques TR, Mehta MA, O'Gorman R, Alsop DC, Taylor H, Johnston A, Williams S, McGuire P, Pariante CM, Kapur S, Dazzan P (2013) Acute effects of single-dose aripiprazole and haloperidol on resting cerebral blood flow (rCBF) in the human brain. Hum Brain Mapp 34:272–282.

Kapur S, Seeman P (2002) NMDA receptor antagonists ketamine and PCP have direct effects on the dopamine D(2) and serotonin 5-HT(2)receptors-implications for models of schizophrenia. Mol Psychiatry 7:837–844.

Kaufman J, Sullivan GM, Yang J, Ogden RT, Miller JM, Oquendo MA, Mann JJ, Parsey RV, DeLorenzo C (2015) Quantification of the serotonin 1A receptor using PET: Identification of a potential biomarker of major depression in males. Neuropsychopharmacology 40:1692–1699.

Kraemmer J, Kovacs GG, Perju-Dumbrava L, Pirker S, Traub-Weidinger T, Pirker W (2014) Correlation of striatal dopamine transporter imaging with post mortem substantia nigra cell counts. Mov Disord 29:1767–1773.

Krystal AD, Weiner RD (1999) EEG correlates of the response to ECT: a possible antidepressant role of brain-derived neurotrophic factor. J ECT 15:27–38.

Kuczenski R, Segal D (1989) Concomitant characterization of behavioral and striatal neurotransmitter response to amphetamine using in vivo microdialysis. J Neurosci 9:2051–2065.

Logothetis NK (2008) What we can do and what we cannot do with fMRI. Nature 453:869–878.

Markowitz JS, DeVane CL, Ramamoorthy S, Zhu H-J (2009) The psychostimulant d-threo-(R, R)-methylphenidate binds as an agonist to the 5HT1A receptor. Pharm- Int J Pharm Sci 64:123–125.

Matthews PM, Honey GD, Bullmore ET (2006) Applications of fMRI in translational medicine and clinical practice. Nat Rev Neurosci 7:732–744.

Mendlin A, Martin FJ, Jacobs BL (1999) Dopaminergic input is required for increases in serotonin output produced by behavioral activation: an in vivo microdialysis study in rat forebrain. Neuroscience 93:897–905.

Moghaddam B, Adams B, Verma A, Daly D (1997) Activation of Glutamatergic Neurotransmission by Ketamine: A Novel Step in the Pathway from NMDA Receptor Blockade to Dopaminergic and Cognitive Disruptions Associated with the Prefrontal Cortex. J Neurosci 17:2921–2927.

Mu Q, Johnson K, Morgan PS, Grenesko EL, Molnar CE, Anderson B, Nahas Z, Kozel FA, Kose S, Knable M, others (2007) A single 20 mg dose of the full D 1 dopamine agonist dihydrexidine (DAR-0100) increases prefrontal perfusion in schizophrenia. Schizophr Res 94:332–341.

Palomero-Gallagher N, Amunts K, Zilles K (2015) Transmitter Receptor Distribution in the Human Brain. In: Brain Mapping: An Encyclopedic Reference, pp 261–275. Elsevier.

Paterson LM, Kornum BR, Nutt DJ, Pike VW, Knudsen GM (2013) 5-HT radioligands for human brain imaging with PET and SPECT. Med Res Rev 33:54–111.

Petcharunpaisan S, Ramalho J, Castillo M (2010) Arterial spin labeling in neuroimaging. World J Radiol 2:384–398.

Roffman JL, Tanner AS, Eryilmaz H, Rodriguez-Thompson A, Silverstein NJ, Ho NF, Nitenson AZ, Chonde DB, Greve DN, Abi-Dargham A, others (2016) Dopamine D1 signaling organizes network dynamics underlying working memory. Sci Adv 2:e1501672.

Rorden C, Brett M (2000) Stereotaxic display of brain lesions. Behav Neurol 12:191–200.

Schouw MLJ, Kaag AM, Caan MW, Heijtel DFR, Majoie CB, Nederveen AJ, Booij J, Reneman L (2013) Mapping the hemodynamic response in human subjects to a dopaminergic challenge with dextroamphetamine using ASL-based pharmacological MRI. Neuroimage 72:1–9.

Seah S, Asad ABA, Baumgartner R, Feng D, Williams DS, Manigbas E, Beaver JD, Reese T, Henry B, Evelhoch JL, others (2014) Investigation of Cross-Species Translatability of Pharmacological MRI in Awake Nonhuman Primate-A Buprenorphine Challenge Study. PloS One 9:e110432.

Shmueli K, van Gelderen P, de Zwart JA, Horovitz SG, Fukunaga M, Jansma JM, Duyn JH (2007) Low-frequency fluctuations in the cardiac rate as a source of variance in the resting-state fMRI BOLD signal. NeuroImage 38:306–320.

Singh KD (2012) Which “neural activity” do you mean? fMRI, MEG, oscillations and neurotransmitters. Neuroimage 62:1121–1130.

Thase ME, Larsen KG, Reines E, Kennedy SH (2013) The cardiovascular safety profile of escitalopram. Eur Neuropsychopharmacol 23:1391–1400.

Volkow ND, Wang G-J, Fowler JS, Molina PE, Logan J, Gatley SJ, Gifford A, Ding Y-S, Wong C, Pappas NR, others (2003) Cardiovascular effects of methylphenidate in humans are associated with increases of dopamine in brain and of epinephrine in plasma. Psychopharmacology (Berl) 166:264–270.

Wang DJJ, Chen Y, Fernández-Seara MA, Detre JA (2011) Potentials and Challenges for Arterial Spin Labeling in Pharmacological Magnetic Resonance Imaging. J Pharmacol Exp Ther 337:359–366.

Wise RG, Preston C (2010) What is the value of human FMRI in CNS drug development? Drug Discov Today 15:973–980.

Wu W-C, Edlow BL, Elliot MA, Wang J, Detre JA (2009) Physiological modulations in arterial spin labeling perfusion magnetic resonance imaging. IEEE Trans Med Imaging 28:703–709.

Zanos P et al. (2016) NMDAR inhibition-independent antidepressant actions of ketamine metabolites. Nature 533:481–486.

Table 1 Study data and medication details

	Compound							
	Risperidone	**Olanzapine**	**Haloperidol**	**Methyl-phenidate (Ritalin)**	**Escitalopram (Lexapro)**	**Ketamine**	**Midazolam**	**Test-retest**
N subjects	21	21	21	18	18	26	26	29
Study ID	1	2	2	3	3	4	4	5
Demo-graphics (n male, age±SD)	21, 28±7	21, 28±6	21, 28±6	9, 25±8	9, 25±8	26, 26±5	26, 26±5	7, 25±6
ASL acquisitions per session (N)	2	2	2	1	1	1	1	1
Location	KCL	KCL	KCL	UCSD	UCSD	UA	UA	UG
Dose (in mg)	0.5 and 2	7.5	3	30	20	0.25 mg/kg (bolus), 0.25 mg/kg/hr (infusion)	0.03 mg/kg (bolus, 0.03 mg/kg/hr (infusion)	-
Scanning time (post adminstration)	2h	5h	5h	4h	4h	0h*	0h*	-
T-max	1.3h	4h	6h	4.7h	5h	-	-	-
Primary drug indication	SZ, Bipolar	SZ, Bipolar	SZ, Bipolar, Tourette syndrome, Mania	ADHD	Depression, anxiety disorders	Anesthesia, chronic pain	Anesthesia	-
Mechanism of action	Direct receptor binding	Direct receptor binding	Direct receptor binding	Reuptake inhibitor	Reuptake inhibitor	Direct receptor binding and reuptake inhibitor	Positive allosteric modulator	-
Agonist effects	-	-	-	Dopamine, catecholamines, (serotonin)	Serotonin	Dopamine, neuroepinephrine, serotonin	GABA	-
Antagonist effects	Dopamine, serotonin, catecholamines	Dopamine, serotonin, catecholamines	Dopamine, serotonin, catecholamines	-	-	Glutamate, acetylcholine	-	-
Receptors	D1-4, 5-HT 1a and 2a, α1, α2	D1,D2,D4, 5-HT 1, 2a and 3, D1, α1, α2, muscarinic, H1	D1-3, 5-HT 2a, α1, σ1	DAT, NET, SERT	SERT	NMDA, D2, 5-HT 2, AMPA, MAT, nicotinic a4b2, muscarinic	BZD	-
Highest affinity to	D2, 5-HT 2a, D3, α2	5-HT 2a, D2	D2, D3	-	-	NMDA	BZD	-

ADHD – Attention Deficit Hyperactivity Disorder, AMPA - , ASL – Arterial Spin Labeling, BZD – Benzodiazepine, DAT – dopamine transporter, GABA - Gamma-Amino butyric acid, KCL – King's College London, MAT – monoamine transporter, NET – norepinephrine transporter, NMDA - N-methyl-D-aspartate receptor, SERT – serotonin transporter, SZ – Schizophrenia, UCSD – University of California San Diego, UA – University of Auckland, UG – University of Groningen, * intravenous infusion

Fig. 1 Schematic overview of the proposed mapping of cerebral blood flow (CBF) changes to underlying receptor densities, activity and affinities

Fig. 2 Results of Pearson correlation, multiple linear regression and effect size analyses. a) Results of Pearson correlation (left) and multiple linear regression analyses between receptor densities and CBF changes are displayed as bar plots. For drugs with only one evaluated dose the drug profiles are colored as "high dose". Red line for Pearson correlation plots indicates significance at an uncorrected two-sided $p<.05$ and yellow star indicates significant Bonferroni corrected findings, For multiple linear regressions a plus indicates a marginally significant ($p<.1$) and red star a significant ($p<.05$) effect of the corresponding regressor. b) Voxel-wise effect size maps (Cohen's d) are displayed for drug treatments matching the order of drugs displayed in a). For risperidone the outcomes for the high dose are displayed.

Fig. 3 Results of correlational analyses with molecular imaging based receptor density estimates and affinities. a) Correlational plots between regional cerebral blood flow (CBF) changes and respective dopamine transporter (DAT) density profiles are displayed for each drug with dopaminergic mechanism of action. b) DAT density estimates obtained from a healthy volunteer cohort provided by the Parkinson's Progression Marker Initiative. c) Correlational plot between midazolam induced CBF changes and GABAa density estimates obtained from flumazenil positron emission tomography. d) Correlations of cerebral blood flow (CBF) changes to receptor density profiles with drug affinities. Colors indicate different receptors. Shapes indicate different drugs. Solid line in all plots indicates the linear regression fit.

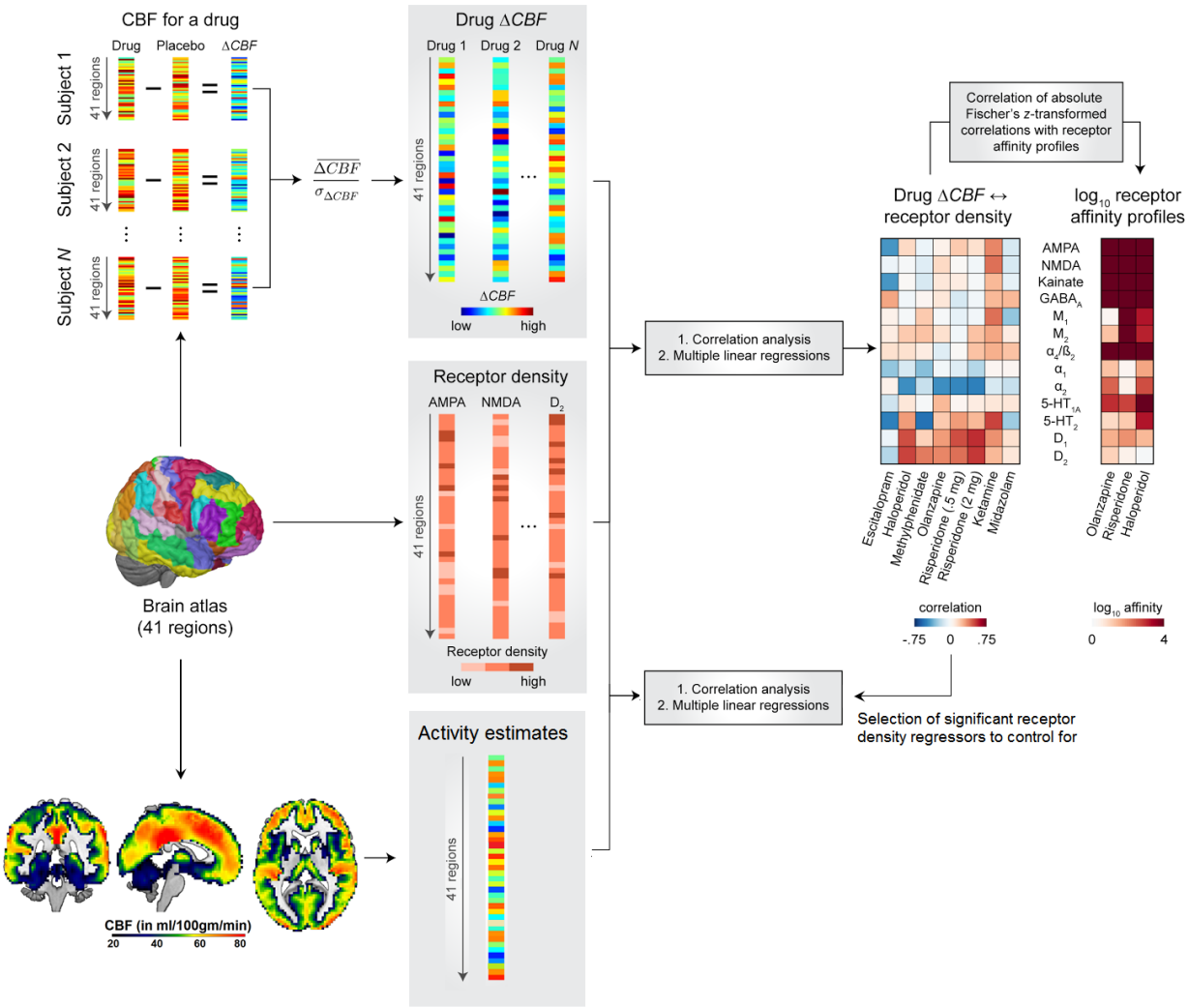
CBF for a drug
Drug
Placebo
ΔCBF
Subject 1
Subject 2
Subject N
41 regions
Drug ΔCBF
Drug 1
Drug 2
Drug N
ΔCBF
low
high
Receptor density
AMPA
NMDA
D2
Brain atlas
(41 regions)
Activity estimates
CBF (in ml/100gm/min)
20
40
60
80
1. Correlation analysis
2. Multiple linear regressions
Correlation of absolute Fischer's z-transformed correlations with receptor affinity profiles
Drug ΔCBF ↔ receptor density
log10 receptor affinity profiles
AMPA
NMDA
Kainate
GABAA
M1
M2
α2/ß2
α1
α2
5-HT1A
5-HT2
D1
D2
Escitalopram
Haloperidol
Methylphenidate
Olanzapine
Risperidone (.5 mg)
Risperidone (2 mg)
Ketamine
Midazolam
Olanzapine
Risperidone
Haloperidol
correlation
-.75
0
.75
log10 affinity
0
4
Selection of significant receptor density regressors to control for

[Figure 1]

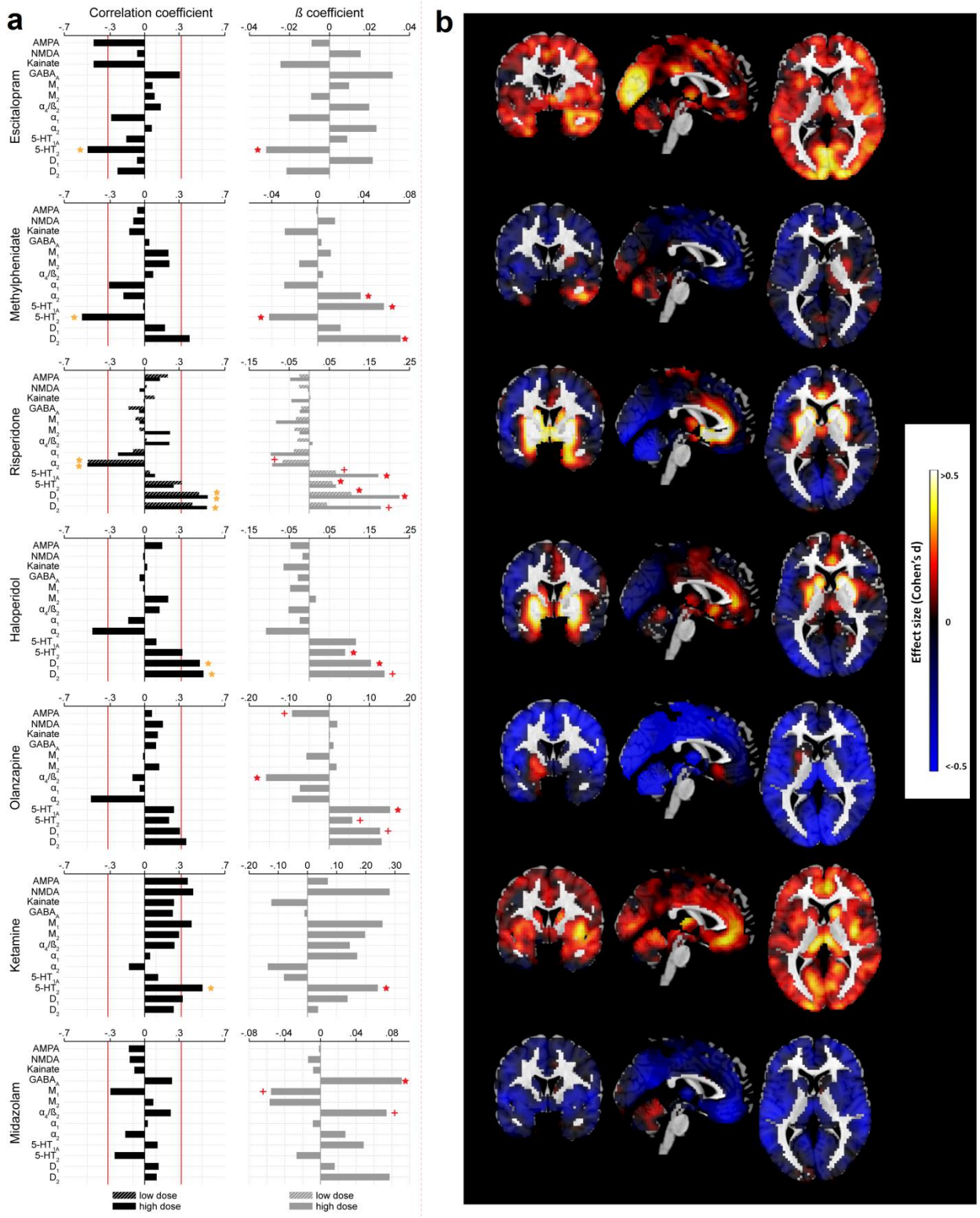
a
Correlation coefficient
ß coefficient
Escitalopram
Methylphenidate
Risperidone
Haloperidol
Olanzapine
Ketamine
Midazolam
AMPA
NMDA
Kainate
GABA$_A$
M$_1$
M$_2$
α$_4$/ß$_2$
α$_1$
α$_2$
5-HT$_{1A}$
5-HT$_2$
D$_1$
D$_2$
low dose
high dose
b
Effect size (Cohen's d)
>0.5
0
<-0.5

[Figure 2]

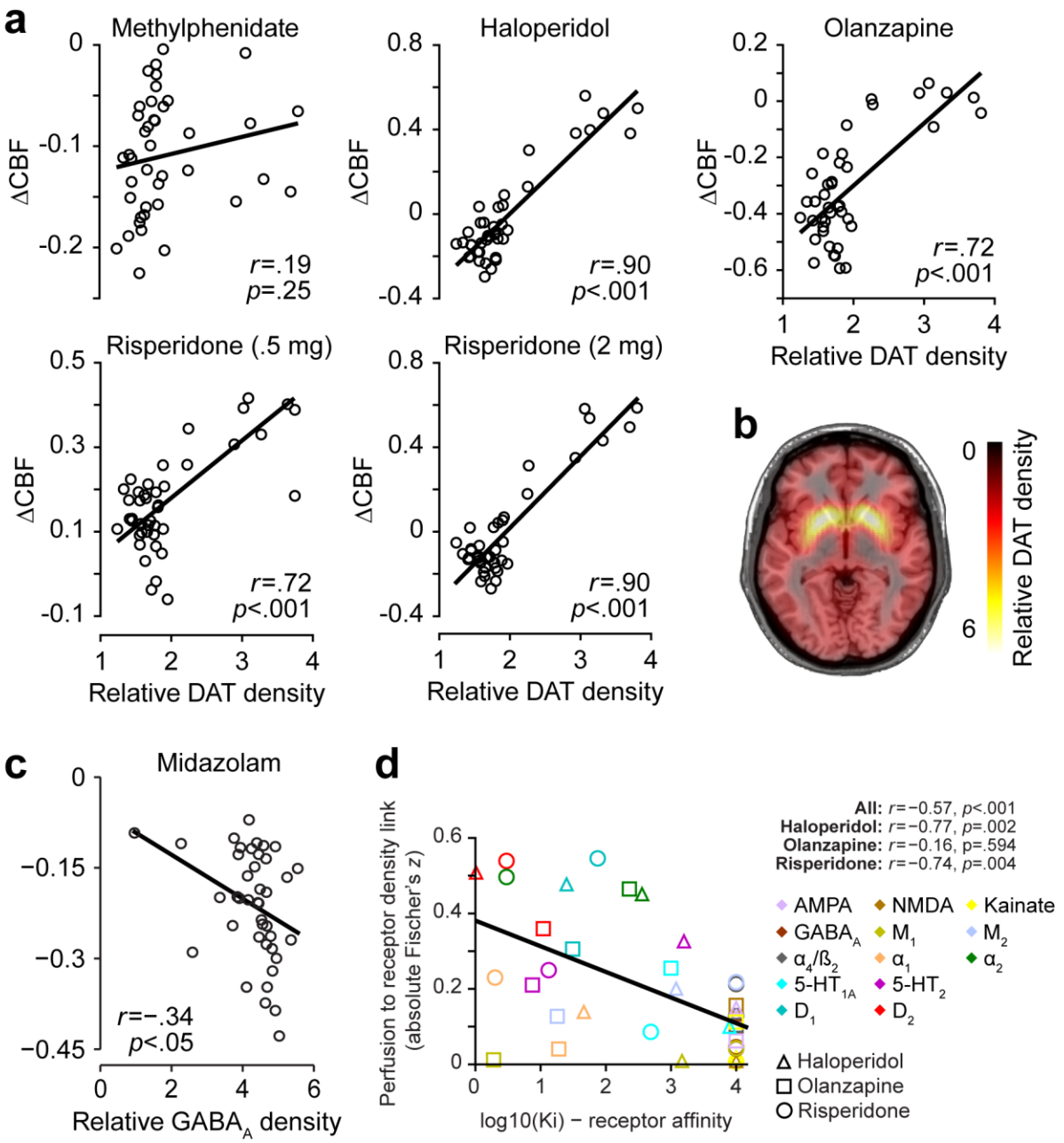
a
Methylphenidate
Haloperidol
Olanzapine
Risperidone (.5 mg)
Risperidone (2 mg)
ΔCBF
r=.19
p=.25
r=.90
p<.001
r=.72
p<.001
r=.72
p<.001
r=.90
p<.001
Relative DAT density
b
Relative DAT density
c
Midazolam
r=−.34
p<.05
Relative GABA_A density
d
Perfusion to receptor density link (absolute Fischer's z)
log10(Ki) − receptor affinity
All: r=−0.57, p<.001
Haloperidol: r=−0.77, p=.002
Olanzapine: r=−0.16, p=.594
Risperidone: r=−0.74, p=.004
AMPA
NMDA
Kainate
GABA_A
M_1
M_2
α_4/ß_2
α_1
α_2
5-HT_1A
5-HT_2
D_1
D_2
Haloperidol
Olanzapine
Risperidone

[Figure 3]